Fabrication of open-ended high aspect-ratio anodic TiO_2 nanotube films for photocatalytic and photoelectrocatalytic applications†

Chin-Jung Lin,[ab] Wen-Yueh Yu,[ab] Yen-Tien Lu[ab] and Shu-Hua Chien*[ab]

Received (in Cambridge, UK) 13th August 2008, Accepted 12th September 2008
First published as an Advance Article on the web 14th October 2008
DOI: 10.1039/b813937g

A facile process is introduced to flake high aspect-ratio anodic TiO_2 nanotube (TiNT) arrays off Ti substrates and then chemically remove the bottom caps to obtain open-ended TiNT films that exhibit high activity to photocatalytic degradation of methylene blue and efficient hydrogen production from photoelectrocatalytic water splitting.

Ordered arrays of one-dimensional (1-D) architectures in a variety of semiconducting materials have attracted significant interest due to their impressive properties for applications in the fields of photocatalytic degradation of pollutants,[1–3] hydrogen generation from photoelectrocatalytic water splitting,[4–6] dye-sensitized solar cells,[7–9] gas sensors,[10] and their being hard templates for the fabrication of well-defined nanostructures.[9,11] The tubular structure, providing availability of both the internal and external areas of the nanotubes for reaction, has been recognized to be preferable because these applications are mostly surface area controlled. Growth of highly ordered TiO_2 nanotube (TiNT) arrays with a length of a few hundred nanometres has been first reported using electrochemical anodization of Ti foil in aqueous hydrofluoric acid solution.[12,13] Recently, very high aspect-ratio TiNT arrays grown up to hundreds of micrometres in length were obtained through anodization of Ti foil in non-aqueous organic electrolytes.[14] However, the nature of TiNT arrays attached to an opaque Ti foil and with a closed bottom has restricted their feasibility for use in extensive applications due to the incident light direction and mass transport of reactants/products.

Grimes and co-workers[15] have reported the detachment of the TiNT film from the underlaying Ti substrate using ultrasonic agitation. A dilute hydrofluoric acid and sulfuric acid solution was used to chemically etch the barrier layer for opening the closed bottom of the tube. Albu *et al.*[16] used selective dissolution of the Ti substrate in $CH_3OH–Br_2$ solution for obtaining a free-standing closed-ended TiNT film and then removed the bottom of the TiNT film by exposing it to HF vapor.

In this present work, we introduce a simple, cost-effective and environment-friendly method with more handy experimental procedures to obtain free-standing open-ended high aspect-ratio anodic TiNT films. The resulting open-ended structure allows the photons and the reactants easy access to the nanotube-array surface as well as superior electron-collecting efficiency, leading to high photocatalytic activities to degradation of methylene blue and efficient hydrogen production from solar water splitting.

The whole process for fabricating the free-standing open-ended TiNT film is sketched in Fig. 1. The process starts with the preparation of high aspect-ratio TiNT arrays on Ti foil (TiNT/Ti)[17] using the electrochemical anodization of Ti foil at 80 V in an electrolyte composed of 0.5 wt% NH_4F and 3 wt% concentrated H_2O_2 solution in ethylene glycol for 24 h. Subsequently, the resulting TiNT/Ti was immersed in 33 wt% H_2O_2 solution for 20 s, so that the lifting of the entire TiNT film off the Ti foil was easily achieved, as shown in Fig. 2. The average inner diameter of the nanotube is 130 nm with a wall thickness of 25 nm and the tube length is 256 μm (as shown in the insets of Fig. 2), corresponding to a high aspect ratio of ~1420. It is clear that tube-pore mouths are open at the top of the TiNT while being closed at the bottom. Here, we use oxalic acid to remove the bottom caps. During the wet-chemical etching, a thin layer of hot-melt adhesive was used as a protective layer to cover on the top mouths of the TiNT film for retaining its tubular structure. The free-standing TiNT film was then immersed in the 0.5% oxalic acid solution at 40 °C for a certain time. Finally, the thin protective layer was separated from the TiNT film by soaking in acetone solution at 60 °C for 2 h. The FE-SEM images of the bottom view of the TiNT film with treatment times of 0, 2, 8 and 16 h are

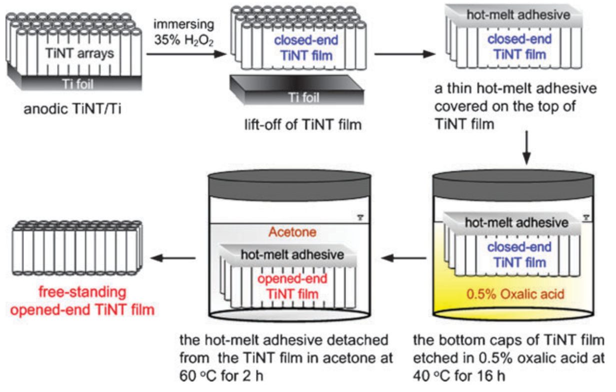

Fig. 1 Scheme for fabricating free-standing open-ended TiNT films.

---

[a] *Institute of Chemistry, Academia Sinica, Taipei 11529, Taiwan. E-mail: chiensh@gate.sinica.edu.tw*
[b] *Department of Chemistry, National Taiwan University, Taipei 10617, Taiwan*

† Electronic supplementary information (ESI) available: X-Ray diffraction profiles of the annealed TiO_2 nanotube film and the sol–gel processed TiO_2 nanoparticles; SEM image of the side-view of the TiNT/FTO electrode; current density–potential characteristics for water splitting using the NP-TiO_2/FTO electrode in the dark and under AM 1.5G illumination. See DOI: 10.1039/b813937g

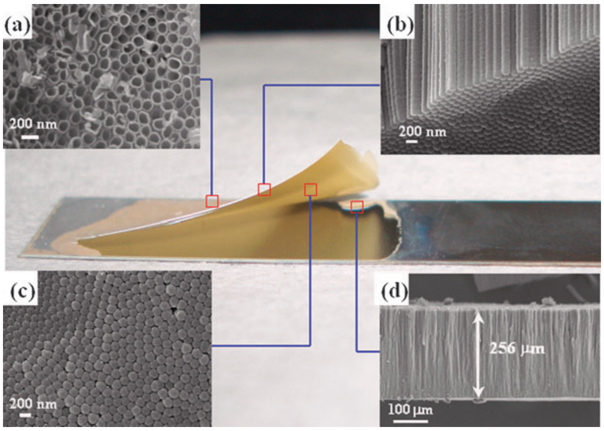

Fig. 2 Photograph of the TiNT arrays after immersion in 33% H_2O_2 for 20 s. The insets are FE-SEM images of the (a) top view; (b) side-view and (c) bottom view. The thickness of the TiNT arrays is shown in (d).

shown in Fig. 3(a)–(d). The caps of the tube bottoms were gradually removed and finally fully opened. Titanium oxide located in the interconnection of the tube and the bottom caps was mainly etched by oxalic acid to form a yellow titanium oxalate complex into the solution. Thus, the bottom caps gradually fell off the tube bottoms and open pores appeared. The ordered tubular structure still remained intact, as can be seen by comparing the images shown in the insets of Fig. 3(a) and (d). The optical images of the closed-ended and the open-ended TiNT films are also displayed in the insets of Fig. 3(a) and (d), in which the TiNT films were placed atop the letters "TiNT" written on white paper. When a white LED light was used to cause illumination through the white paper, the "TiNT" letters can be identified for the open-ended TiNT film as being optically transparent, while, the closed-ended TiNT film is optically translucent. After annealing in oxygen at 500 °C for 3 h, the TiNT films were transformed to the anatase phase of TiO_2, appearing white in color (see ESI,† Fig. S1).

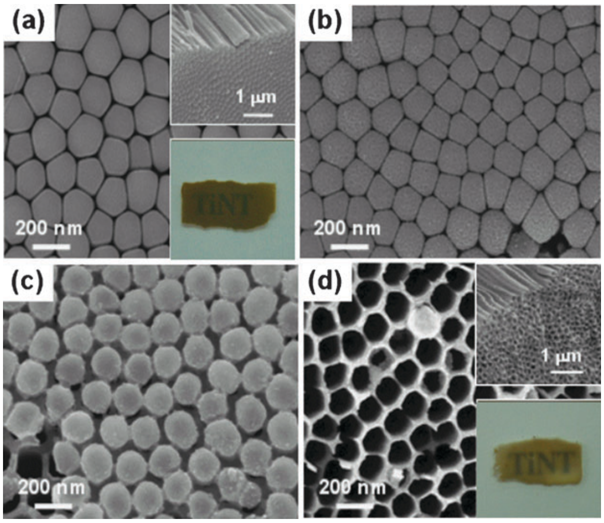

Fig. 3 FE-SEM bottom view images of the evolution of the TiNT films after immersing in the 0.5% oxalic acid solution for (a) 0 h; (b) 2 h; (c) 8 h and (d) 16 h. The insets are FE-SEM side-view images and optical images.

Photocatalytic performances of the closed-ended and the open-ended TiNT films were evaluated *via* bleaching methylene blue solution by UV irradiation. The 256 μm long closed-ended and the open-ended TiNT films with active areas of about 1 cm^2 were placed vertically in a quartz cell ($1 \times 1 \times 4.5$ cm^3) containing 3 mL of 10 mg L^{-1} methylene blue, sealed with a rubber stopper, and put inside a Rayonet RPR-100 Photoreactor equipped with sixteen UV lamps (350 nm). The concentration of methylene blue in the solution was measured using UV-Vis spectroscopy according to the intensity of the 665 nm absorption peak. A blank test indicates that the decoloration of the dye solution is negligible in the absence of TiO_2 photocatalyst within an irradiation period of 5 h. The TiNT film was immersed in the methylene blue solution and kept in the dark for 30 min, and then the UV light was turned on. Fig. 4 shows the time profiles of C/C_0 for the experiments with the open-ended and closed-ended TiNT films, where C is the concentration of methylene blue at the irradiation time t, C_0 is the initial concentration. A first-order rate model, $-dC/dt = k_{obs} \times C$, effectively describes the photocatalytic decoloration of the methylene blue solution, where k_{obs} is the observed rate constant. The complete decoloration of methylene blue solution with the open-ended TiNT film was achieved within 4 h. The resulting values of k_{obs} are 0.21 h^{-1} and 0.28 h^{-1} for the closed-ended TiNT and the open-ended TiNT films, respectively. The 30% difference in the photocatalytic activity might be ascribed to the drawbacks of the bottom caps. (1) The cap acted as a barrier not only to absorb photons but also to reflect the incident light that allowed less effective photons for photocatalysis. (2) With the cap sealing one end of the tube, air might be trapped inside the tube due to surface tension of the solution that made inner surface of the tube less accessible to the methylene blue.

Photoelectrocatalytic generation of hydrogen through water splitting using solar energy offers a potentially clean and renewable fuel source. In this study, we used a TO_2 paste, an aqueous solution containing sol–gel processed TiO_2 nanoparticles (NP-TiO_2) and polyethylene glycol, to adhere the

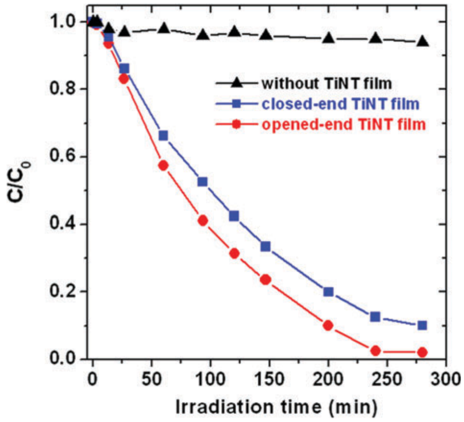

Fig. 4 Photocatalytic degradation kinetics of methylene blue using the open-ended and closed-ended TiNT films. The blank experiment is also shown.

TiNT film onto the fluorine-doped tin oxide (FTO)-coated glass. After annealing at 450 °C for 30 min, a NP-TiO_2 thin layer formed between the FTO glass and the TiNT film that were strongly interconnected. This unit with the TiNT film attached to FTO glass was used as the working electrode, denoted as TiNT/FTO (see ESI,† Fig. S2). Electrochemical experiments were carried out using a three-electrode configuration with a Pt wire counter electrode and a saturated Ag/AgCl reference electrode. The electrolyte was 1 M KOH solution. The working electrode of the TiNT/FTO was illuminated with AM 1.5 G solar light (Oriel) during a voltage sweep from −1.0 to 0.6 V (*versus* Ag/AgCl) with a sweep rate of 5 mV s^{-1}. The spectral output of the lamp was matched to the standard AM 1.5 G solar spectrum in the region of 350–750 nm (mismatch $<5\%$) by adjusting the light intensity with a monocrystalline Si reference cell equipped with an IR-cutoff filter (KG-5). The photocurrent densities generated from the closed-ended and the open-ended TiNT/FTO are presented in Fig. 5. Obviously, the photocurrent generated with the open-ended TiNT/FTO is much higher than that of the closed-ended TiNT/FTO. For the open-ended TiNT/FTO, the open-circuit potential (E_{ocp}) is −763 mV *vs.* Ag/AgCl, a 70 mV negative shift as compared to closed-ended TiNT/FTO ($E_{\mathrm{ocp}} = -694$ mV). It implies that the closed-ended TiNT/FTO provides additional charge recombination sites and thus reduces E_{ocp}. The photoconversion efficiency (η) of light energy to chemical energy in the presence of an external applied potential is calculated according to $\eta\ (\%) = j_{\mathrm{p}}[(E^{\mathrm{o}}_{\mathrm{rev}} - E_{\mathrm{app}})/I_0] \times 100$. $E^{\mathrm{o}}_{\mathrm{rev}}$ equals 1.23 V, which is the potential corresponding to the Gibbs free energy change per photon in the water splitting reaction. $E_{\mathrm{app}} = E_{\mathrm{meas}} - E_{\mathrm{ocp}}$, the term E_{meas} is the electrode potential (*vs.* Ag/AgCl) of the working electrode. j_{p} is the photocurrent density and I_0 is the intensity of the incident light. The results are depicted in the inset of Fig. 5. A maximum conversion efficiency of 0.70% was obtained with the open-ended TiNT/FTO, which was much higher than the 0.22% efficiency obtained by the closed-ended TiNT/FTO or 0.36% by the NP-TiO_2/FTO electrode (see ESI,† Fig. S3). The volume ratio of the evolved hydrogen and oxygen was nearly 2 : 1, as verified by gas chromatographic analysis. Optical features of the open-ended TiNT made a slightly favorable contribution to the photocurrent, while the significant difference might come from the following two drawbacks of the bottom caps. (1) A electron tunnelling barrier was built that reduced the number of charges reaching the electrode. (2) The cap blocked H^+ diffusion out of the NP-TiO_2 thin layer, which caused more charge recombination. The efficiency of 0.70% with the open-ended TiNT/FTO under AM 1.5 G illumination is higher than that (0.58%) with TiNT/Ti reported by Grimes and co-workers,[18] even being among the highest reported to date for a TiO_2 photoelectrochemical cell.[19]

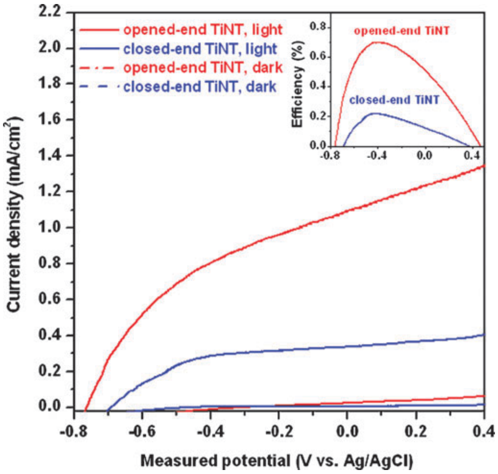

Fig. 5 Current density–potential characteristics for water splitting using the open-ended and closed-ended TiNT films in the dark and under AM 1.5 G illumination (the inset shows the corresponding photoconversion efficiencies).

In summary, a transparent free-standing, high aspect-ratio, open-ended TiNT film was successfully fabricated through flaking the anodic TiNT off the Ti substrate and opening the tube bottom by a facile wet-chemical etching. The originally attracted features of the open-ended TiNT film such as optical transparence and superior electron transport show the enhancement in the photocatalytic and photoelectrocatalytic performances. Extending the photoresponse of this TiNT film to visible light by sensitizing it with narrow band gap semiconductors or dyes is in progress.

We acknowledge the financial supports from Academia Sinica and National Science Council of Taiwan, ROC.

Notes and references

1 Z. P. Zhu, Y. Zhou, H. W. Yu, T. Nomura and B. Fugetsu, *Chem. Lett.*, 2006, **35**, 890.
2 J. J. Wu and C. H. Tseng, *Appl. Catal., B*, 2006, **66**, 51.
3 Z. Liu, X. Zhang, S. Nishimoto, M. Jin, D. A. Tryk, T. Murakami and A. Fujishima, *J. Phys. Chem. C*, 2008, **112**, 253.
4 G. K. Mor, K. Shankar, M. Paulose, O. K. Varghese and C. A. Grimes, *Nano Lett.*, 2005, **5**, 191.
5 Y. Yin, Z. G. Jin and F. Hou, *Nanotechnology*, 2007, **18**, 495608.
6 G. K. Mor, H. E. Prakasam, O. K. Varghese, K. Shankar and C. A. Grimes, *Nano Lett.*, 2007, **7**, 2356.
7 G. K. Mor, K. Shankar, M. Paulose, O. K. Varghese and C. A. Grimes, *Nano Lett.*, 2006, **6**, 215.
8 J. H. Park, T. W. Lee and M. G. Kang, *Chem. Commun.*, 2008, 2867.
9 A. B. F. Martinson, J. W. Elam, J. T. Hupp and M. J. Pellin, *Nano Lett.*, 2007, **7**, 2183.
10 S. Yoriya, H. E. Prakasam, O. K. Varghese, K. Shankar, M. Paulose, G. K. Mor, T. J. Latempa and C. A. Grimes, *Sens. Lett.*, 2006, **4**, 334.
11 J. Qiu, W. Yu, X. Gao and X. Li, *Nanotechnology*, 2006, **17**, 4695.
12 V. Zwilling, E. Darque-Ceretti, A. Boutry-Forveille, D. David, M. Y. Perrin and M. Aucouturier, *Surf. Interface Anal.*, 1999, **27**, 629.
13 D. Gong, C. A. Grimes, O. K. Varghese, W. C. Hu, R. S. Singh, Z. Chen and E. C. Dickey, *J. Mater. Res.*, 2001, **16**, 3331.
14 M. Paulose, K. Shankar, S. Yoriya, H. E. Prakasam, O. K. Varghese, G. K. Mor, T. A. Latempa, A. Fitzgerald and C. A. Grimes, *J. Phys. Chem. B*, 2006, **110**, 16179.
15 M. Paulose, H. E. Prakasam, O. K. Varghese, L. Peng, K. C. Popat, G. K. Mor, T. A. Desai and C. A. Grimes, *J. Phys. Chem. C*, 2007, **111**, 14992.
16 S. P. Albu, A. Ghicov, J. M. Macak, R. Hahn and P. Schmuki, *Nano Lett.*, 2007, **7**, 1286.
17 C. J. Lin, W. Y. Yu and S. H. Chien, *Appl. Phys. Lett.*, 2007, **91**, 233120.
18 M. Paulose, G. K. Mor, O. K. Varghese, K. Shankar and C. A. Grimes, *J. Photochem. Photobiol., A*, 2006, **178**, 8.
19 T. Bak, J. Nowotny, M. Rekas and C. C. Sorrell, *Int. J. Hydrogen Energy*, 2002, **27**, 991.